Density Functional Study of the Structures and Energies of $C_nP_3^-$ ($n = 2-8$) Clusters

M. D. Chen,* L. S. Zheng, and Q. E. Zhang

State Key Laboratory for Physics and Chemistry of Solid Surfaces, Department of Chemistry, Center for Theoretical Chemistry, Xiamen University, Xiamen 361005, People's Republic of China

M. H. Liu and C. T. Au*

Department of Chemistry, Hong Kong Baptist University, Kowloon Tong, Hong Kong, People's Republic of China

Received: June 23, 2003; In Final Form: September 9, 2003

Using molecular graphics software, we have designed numerous models of $C_nP_3^-$ ($n = 2-8$). We carried out geometry optimizations and calculations of vibrational frequency by means of the B3LYP density functional method. After comparing the total energies of the isomers, we found that the ground-state structures are straight carbon chains with a P_2C ring connected at one end and a phosphorus atom at the other. The alternate behavior in electron affinity, bond length, and incremental binding energy with odd and even *n* match the peak pattern observed in the laser-induced mass spectra of $C_nP_3^-$($n = 2-8$). Other than a number of individual isomers, the structures with carbon and phosphorus atoms connected alternately are unstable. Most of the stable models have carbon units in the form of a ring or a chain connecting to different P, P_2, and P_3 units.

1. Introduction

Studies of carbon clusters and compounds have opened up research fields of new dimensions. Recently, experimental and theoretical research on binary clusters has aroused much interest. Compared to the other elements, carbon and phosphorus clusters are more likely to show closed-cage structures. Binary clusters of carbon and nonmetal elements (e.g., O, N, and S) have been discovered in celestial bodies.[1,2] The existence of organophosphorus species in circumstellar and interstellar media is possible.[3] It is known that stable C/P binary anions can be produced by reacting small anionic carbon clusters with gaseous P_4.[4] It has also been reported that C/P binary clusters could be generated by means of unconventional methods such as laser ablation and high-energy electron bombardment.[5−7]

Recently, there have been reports on theoretical investigations of C/P binary clusters. Zhan et al. optimized the geometric structures of C_nP^- ($n = 1-7$) using ab initio calculations.[8] Pascoli et al. proposed structures of C_nP, C_nP^-, C_nP^+ ($n = 1-7$), and $C_nP_p^+$ ($n + p = 3-6$) based on data collected in density functional calculations.[9−11] Using the HF method, Liu et al. carried out calculations on linear C_nP^-($n = 1-11$).[12,13] Fisher et al. conducted density functional calculations on structures of C_nP^-, $C_nP_2^-$, $C_nP_4^-$, and $C_nP_5^-$ ($n = 3-9$) isomers.[4] Zeng et al. analyzed C_nP_2, $C_nP_2^-$, and $C_nP_2^+$ ($n = 3-9$) clusters theoretically by adopting the density functional method.[7] Río et al. investigated various geometries of C_3P and C_3P^+ by ab initio calculations.[14] Largo et al. carried out an ab initio molecular orbital study of C_2P entities and cations.[15] Despite the work that has already been reported on C/P binary clusters, our understanding of these materials is still limited. Until now, no theoretical report on $C_nP_3^-$ binary clusters has been published, and the time-of-flight mass spectra of C/P binary clusters showed distinct peaks of $C_nP_3^-$.[5−7] There is a discrepancy in these experimental results. The mass spectrum reported by Liu et al. (generated in the laser ablation of a mixture of carbon and phosphorus)[5] has $C_nP_3^-$ ($n < 8$) peaks missing (Figure 1). However, the mass spectrum of Zeng et al. showed $C_nP_3^-$ ($2 < n < 8$) peaks for even *n*.[7] In fact, the intensities in mass spectrometry depend mainly on the experimental set up, and the experimental results are generally not completely conclusive. To view the issue theoretically, we designed tens of structural models of $C_nP_3^-$ ($n = 2-8$) and performed geometry optimization and calculations on vibrational frequencies on the basis of the B3LYP density functional method. After comparing the stability of all of the models, we summarized the general patterns and proposed structural rules for $C_nP_3^-$. We found that the $C_nP_3^-$ ($n = 2-8$) isomers with even *n* are more stable than those with odd *n*. The outcome can serve as a helpful guidelines for the synthesis of related materials as well as for future theoretical studies of binary clusters.

2. Computational Method

During the investigation, devices for molecular graphics, molecular mechanics, and quantum chemistry were used. First, a 3D model of a cluster was designed using HyperChem 5.0 for Windows[16] and Desktop Molecular Modeler 3.0 for Windows.[17] Then, the model was optimized in an orderly manner by MM+ molecular mechanics and semiempirical PM3 quantum chemistry. Last, geometry optimization and calculations of vibrational frequencies were conducted using the B3LYP density functional method of Gaussian 98[18] with 6-31G* basis sets. The single-point energy calculations were followed by optimization at a higher level of 6-311+G* basis sets (i.e., B3LYP/6-311+G*//B3LYP/6-31G*).[19] The optimized model was displayed using molecular graphics software. All of the calculations were carried out on a server of PC clusters.

3. Model Constructions

With the molecular graphics software,[16,17] the initial models were constructed by breaking bonds, making bonds, adding

* Corresponding authors. E-mail: pctau@hkbu.edu.hk.

10.1021/jp035790o CCC: $25.00
Published on Web 10/24/2003

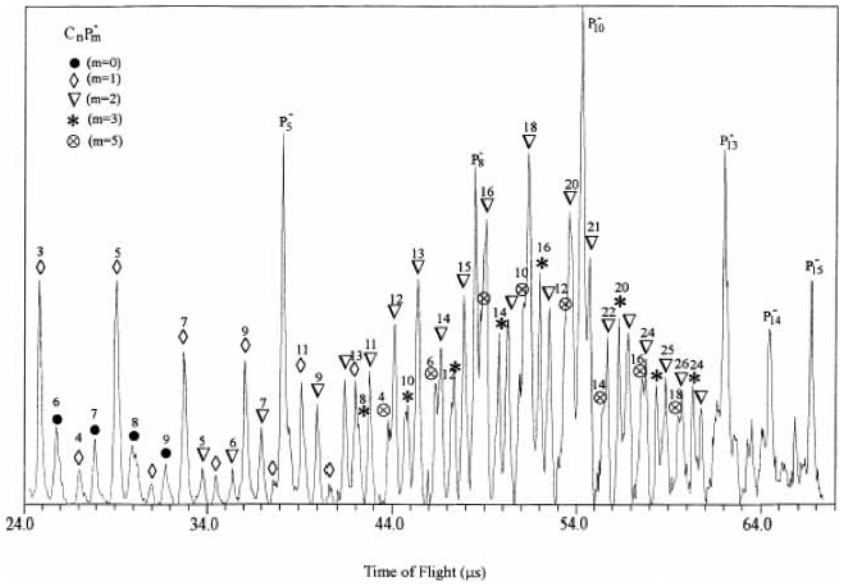

Figure 1. Time-of-flight mass spectrum of $C_nP_m^-$ binary cluster anions.

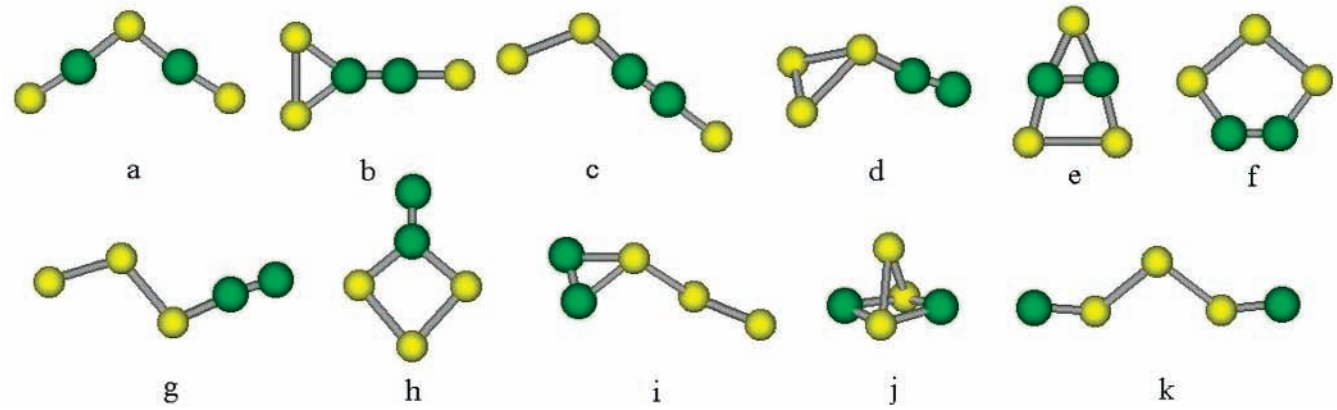

Figure 2. Eleven isomers of $C_2P_3^-$.

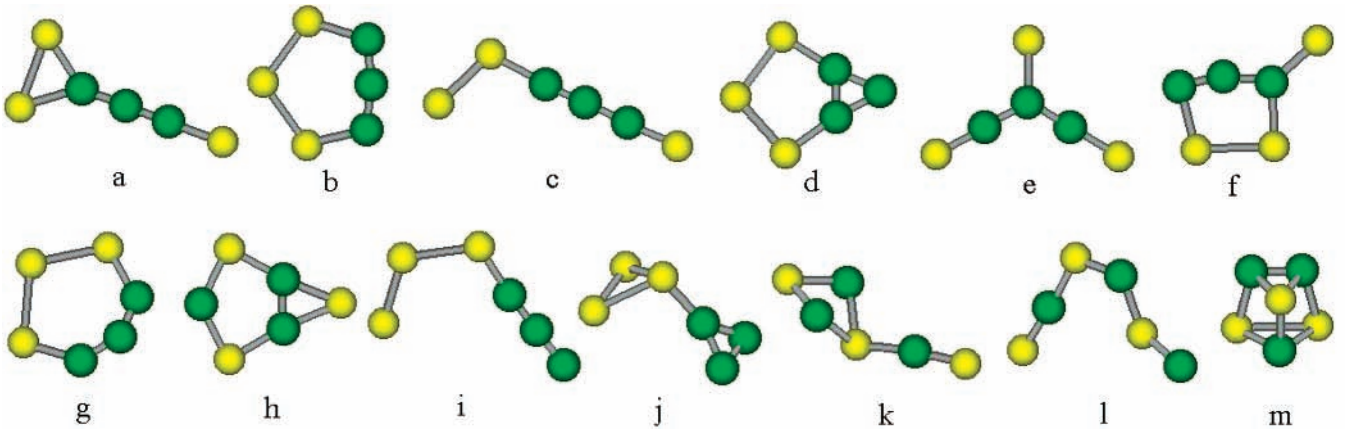

Figure 3. Thirteen isomers of $C_3P_3^-$.

atoms, deleting atoms, rotating fragments, translating fragments, and merging fragments. In Figures 2−8, isomers corresponding to the local minima of $C_nP_3^-$ ($n = 2-8$) with real vibrational frequencies are shown. In each Figure, the models are arranged in order of ascending relative total energy; bigger balls represent carbon atoms, and smaller balls denote phosphorus atoms. Most of the models depicted here have never been reported before. Among the 11 isomers of $C_2P_3^-$ shown in Figure 2, models 2a−c, e−h, and k are planar structures. Displayed in Figure 3 are 13 isomers of $C_3P_3^-$; models 3a−i and l are planar structures. Shown in Figure 4 are 14 isomers of $C_4P_3^-$; models 4a−g and j are planar in structure. Displayed in Figure 5 are nine isomers of $C_5P_3^-$; models 5a−f are planar structures. Among the 10 isomers of $C_6P_3^-$ shown in Figure 6, models 6a−g are planar structures. Shown in Figure 7 are nine isomers of $C_7P_3^-$. The planar structures of models 7a−g exhibit the same structural characteristic of the corresponding models (5a−g) in Figure 5, having two carbon atoms added to the respective carbon units. Except for the models of the ground and second most stable state, the order of listing in Figure 7 is different from that in

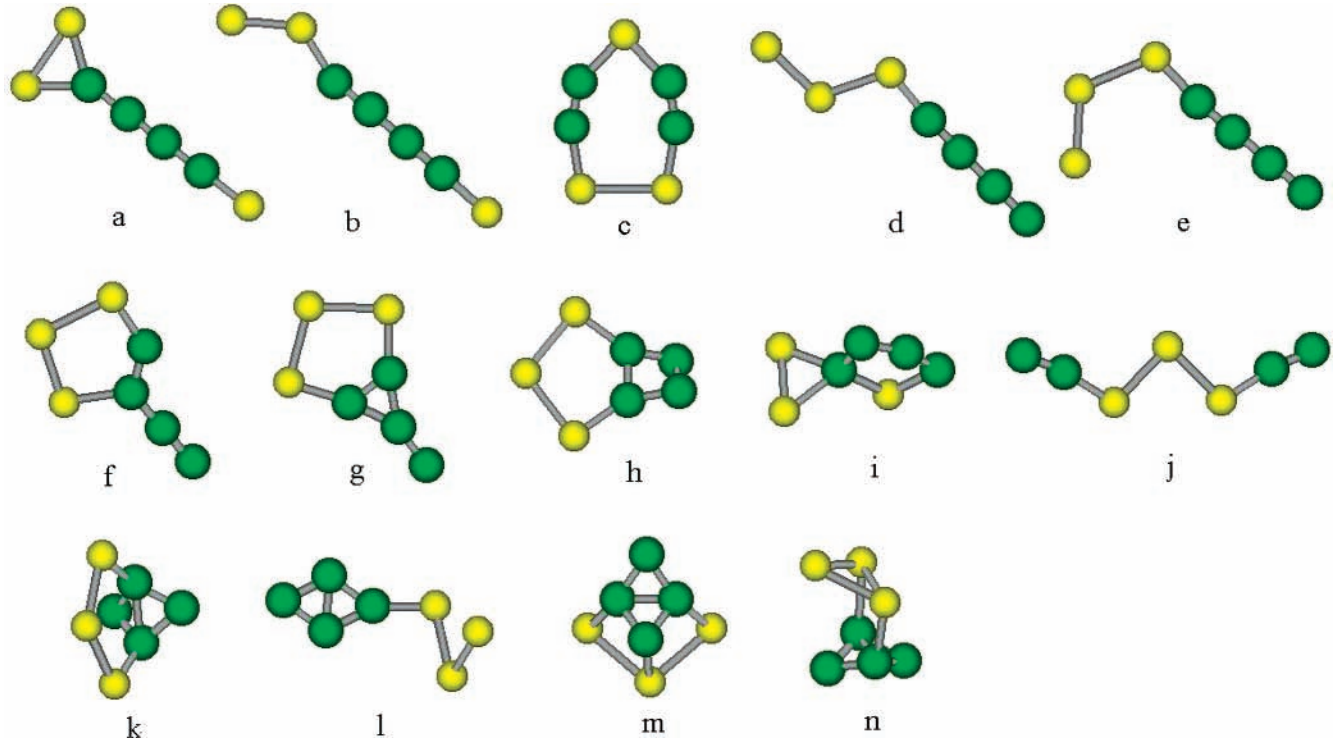

Figure 4. Fourteen isomers of $C_4P_3^-$.

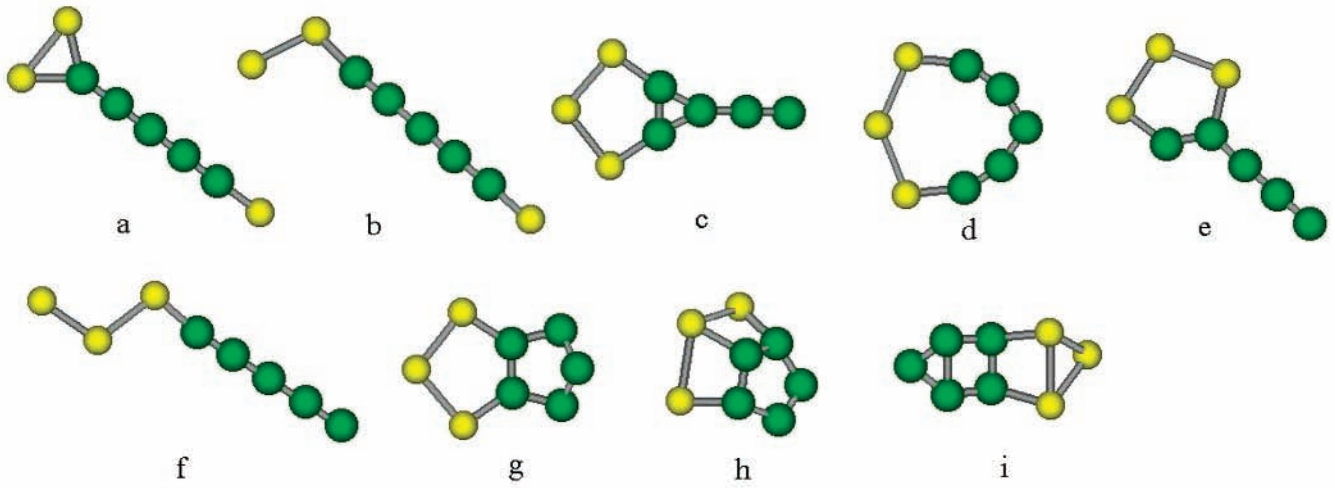

Figure 5. Nine isomers of $C_5P_3^-$.

Figure 5. Displayed in Figure 8 are 13 isomers of $C_8P_3^-$. Models 8a−g are the results of optimization after adding a C_2 unit to the carbon chains of the corresponding models shown in Figure 6. These are all planar structures.

4. Results and Discussion

Listed in Table 1 are the symmetries, electronic states, and relative energies obtained at the B3LYP/6-311+G* level for the $C_nP_3^-$($n = 2-8$) isomers shown in Figures 2−8. In all cases of $C_nP_3^-$ clusters, spin contamination $\langle S^2 \rangle$ is between 2.01 and 2.07. Being smaller than 4% in deviation, it will not affect the results severely. For ground-state $C_nP_3^-$ clusters, the energy differences between singlet and triplet states are found to be at least 0.59 eV, big enough to prevent errors in state ordering. Because of the fact that there are numerous isomers in the structures of clusters, the identification of the ground state is important. For a particular family of molecules, the basic structure with the lowest energy affects the "building up" of larger molecules, and this is a vital area in biochemical research. According to the relative total energies listed in Table 1, model 2a is the $C_2P_3^-$ structure with the lowest energy; it is "V" shaped, and the C and P atoms are connected alternately. The 2b structure is the second lowest in energy and shows a P_2C ring connected to a CP chain via C−C bonding. Model 3a is the $C_3P_3^-$ structure with the lowest energy; it is a six-membered ring formed by joining a P_3 with a C_3 unit. Model 3b is the optimized result of increasing the carbon chain of 2b by one atom; the total energy of 3b is only 0.06885 eV higher than that of 3a. When employing B3LYP/6-31G* energies, model 3b is slightly more stable than model 3a. It is apparent that a difference in theoretical levels in calculations of structures with similar energies could result in different energy ordering. We consider that both models are candidates for the ground-state $C_3P_3^-$ structure. The most stable structures of $C_nP_3^-$ ($n = 4-8$)

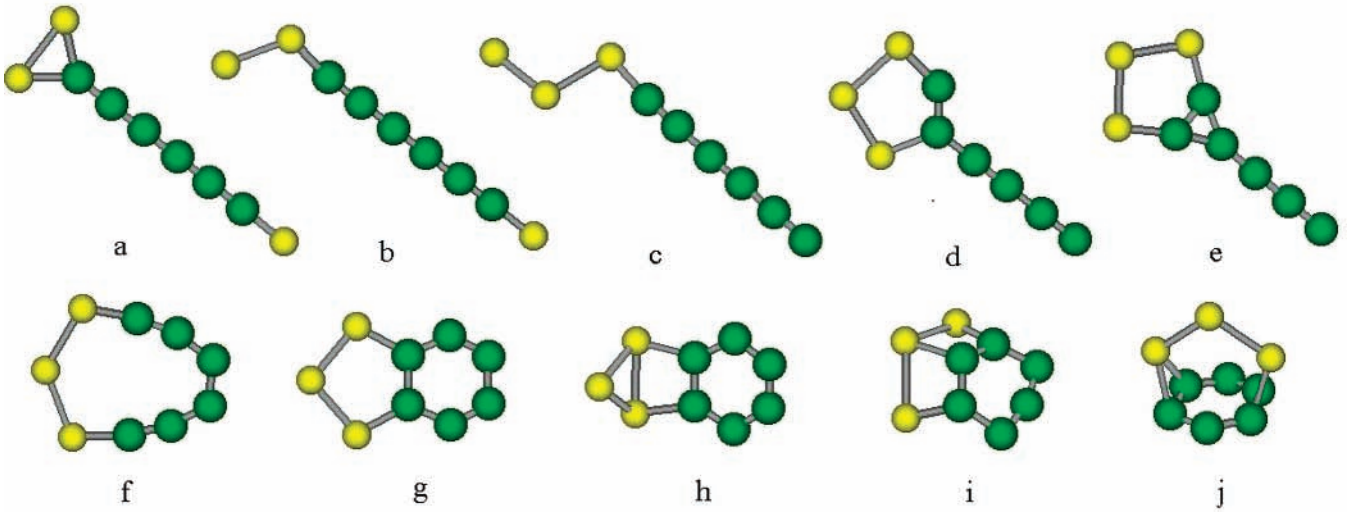

Figure 6. Ten isomers of $C_6P_3^-$.

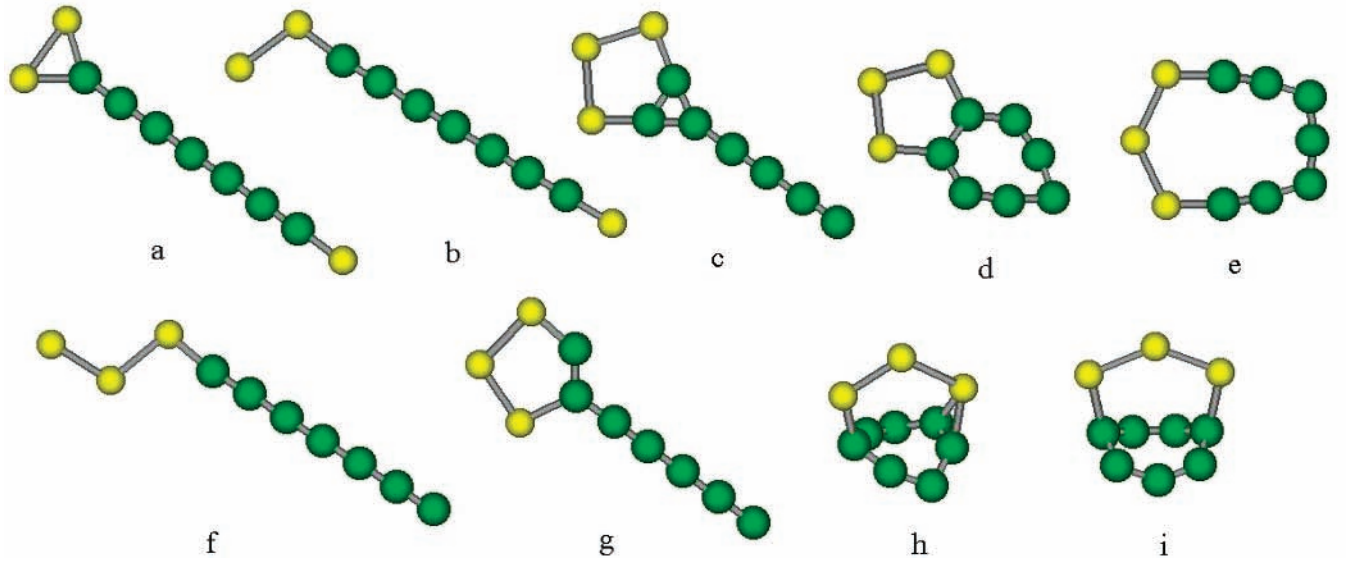

Figure 7. Nine isomers of $C_7P_3^-$.

can be regarded as the outcomes of increasing the carbon chain of 3b, with one phosphorus atom located at one end and a P_2C ring at the other. The structures of C_n and C_n^- ($n < 14$) clusters are usually linear or cyclic in structure.[20] It has been pointed out that the most stable structures of C_nP^- are linear as well,[8,9,12,13] with the phosphorus atom located at one end of the chain. The most stable structures of C_nP_2 and $C_nP_2^-$ are also linear,[4,7] with one phosphorus atom located at each end of the carbon chain. According to the results of our calculation, with $C_2P_3^-$ being an exception, the most stable structures of $C_nP_3^-$ are not linear because at one end of the straight carbon chain is a P_2C three-membered ring. Furthermore, the energy of the triplet state is always the lowest. We find that because of a delocalized π bond, there is a reduction in total energy. The most stable structures are planar and subject to C_{2v} symmetry. The p orbitals of the chain carbon atoms overlap to form delocalized π bonds. Within the CP_2 planar ring and the straight chain, the p orbitals of all of the carbons and two phosphorus atoms overlap, and the delocalized cyclic π bond causes a reduction in the total energy. In Figure 9, the $^1b_1$ molecular orbital referred to as a π orbital of $C_3P_3^-$ is depicted. The other models of $C_nP_3^-$ with the structural style of model 2b have π orbitals of a similar nature.

Electron affinity (EA) is computed as the energy difference between the neutral and anionic ($E_{\text{neutral}} - E_{\text{anion}}$) clusters. A higher electron affinity means that more energy is released when an electron is added to the neutral molecule and the production of the corresponding anion is more readily accomplished. Listed in Table 2 are the electron affinities of clusters that display the structural style of model 2b. Shown in Figure 10 is the variation curve of election affinity as related to the number of carbon atoms, *n*, within the clusters. One can see that the EA values of $C_nP_3^-$ with even *n* are higher than those with odd *n*, reflecting an alternate pattern of high and low. This implies that compared to the cases of odd *n* it is easier to add an electron to C_nP_3 with even *n* (i.e., forming $C_2P_3^-$, $C_4P_3^-$, $C_6P_3^-$, and $C_8P_3^-$). Such an odd−even alternate pattern of electron affinity matches the peak profile of the mass spectra well. In the $C_nP_3^-$ mass spectra of Liu et al.[5,6] and Zeng et al.,[7] $C_nP_3^-$ peaks are observed only for even *n*.

Shown in Figure 11 are the bond lengths of $C_nP_3^-$ ($n = 2-8$) clusters that display the structural style of model 2b after

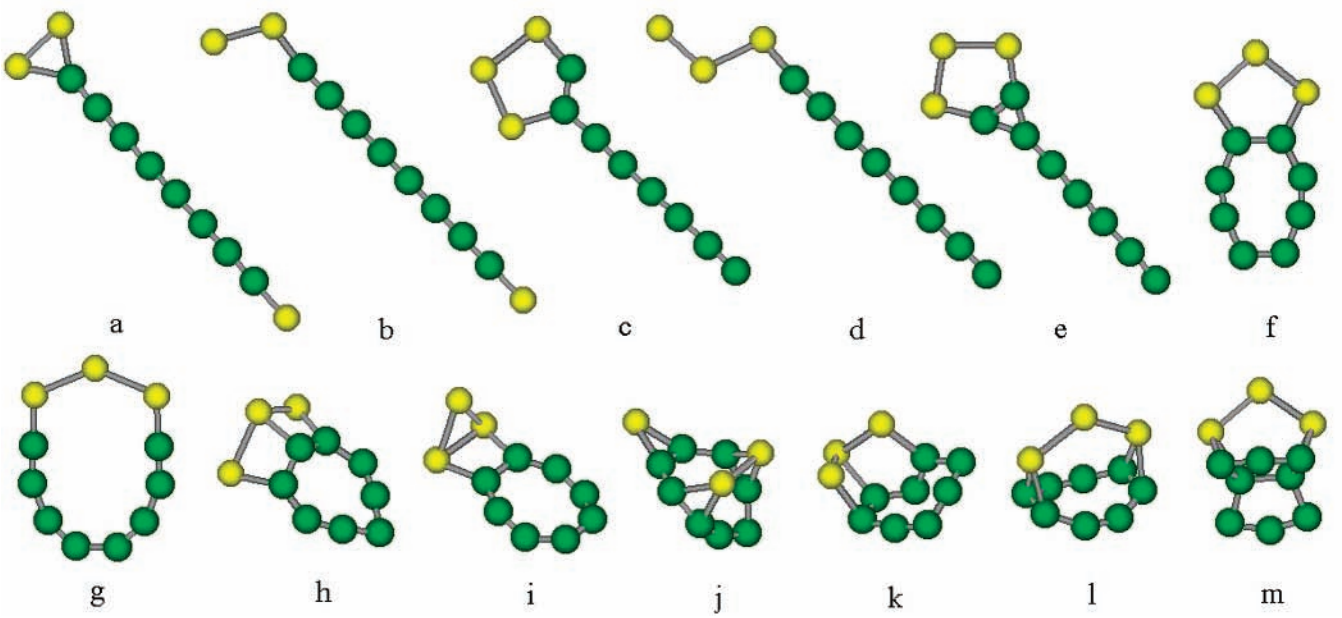

Figure 8. Thirteen isomers of $C_8P_3^-$.

TABLE 1: Symmetries, Electronic States, and Relative Energies (eV) of $C_nP_3^-$ ($n = 2-8$) Isomers Based on B3LYP/6-31G* Geometries and B3LYP/6-311+G* Energies

figure	cluster	symmetry	electronic state	relative energy	figure	cluster	symmetry	electronic state	relative energy
2a	$C_2P_3^-$	C_{2v}	$^1A_1$	0	5a	$C_5P_3^-$	C_{2v}	$^3B_1$	0
2a	$C_2P_3^-$	C_{2v}	$^3B_1$	1.63700	5a	$C_5P_3^-$	C_{2v}	$^1A_1$	0.67772
2b	$C_2P_3^-$	C_{2v}	$^3B_2$	0.24288	5b	$C_5P_3^-$	C_s	$^3A''$	0.14994
2c	$C_2P_3^-$	C_s	$^3A'$	0.82738	5c	$C_5P_3^-$	C_{2v}	$^1A_1$	0.56301
2d	$C_2P_3^-$	C_s	$^1A'$	1.13433	5d	$C_5P_3^-$	C_{2v}	$^3B_1$	2.00032
2e	$C_2P_3^-$	C_{2v}	$^1A_1$	1.45135	5e	$C_5P_3^-$	C_s	$^3A''$	2.24115
2f	$C_2P_3^-$	C_{2v}	$^3B_2$	1.55475	5f	$C_5P_3^-$	C_s	$^3A''$	1.90672
2g	$C_2P_3^-$	C_s	$^3A''$	1.73489	5g	$C_5P_3^-$	C_s	$^1A'$	2.48551
2h	$C_2P_3^-$	C_{2v}	$^3B_1$	2.28865	5h	$C_5P_3^-$	C_s	$^3A''$	3.85534
2i	$C_2P_3^-$	C_{2v}	$^1A_1$	3.04649	5i	$C_5P_3^-$	C_s	$^1A'$	4.42161
2j	$C_2P_3^-$	C_1		3.08377	6a	$C_6P_3^-$	C_{2v}	$^3B_2$	0
2k	$C_2P_3^-$	C_{2v}	$^1A_1$	5.07566	6a	$C_6P_3^-$	C_{2v}	$^1A_1$	0.72525
3a	$C_3P_3^-$	C_{2v}	$^1A_1$	0	6b	$C_6P_3^-$	C_s	$^3A'$	0.59267
3a	$C_3P_3^-$	C_{2v}	$^3A_2$	1.56607	6c	$C_6P_3^-$	C_s	$^3A''$	1.61610
3b	$C_3P_3^-$	C_{2v}	$^3B_1$	0.06885	6d	$C_6P_3^-$	C_s	$^3A''$	1.69583
3b	$C_3P_3^-$	C_{2v}	$^1A_1$	0.88409	6e	$C_6P_3^-$	C_{2v}	$^1A_1$	1.84740
3c	$C_3P_3^-$	C_s	$^3A''$	0.16000	6f	$C_6P_3^-$	C_{2v}	$^3B_2$	2.15434
3d	$C_3P_3^-$	C_{2v}	$^1A_1$	0.28681	6g	$C_6P_3^-$	C_{2v}	$^3B_1$	2.33612
3e	$C_3P_3^-$	C_{2v}	$^3A_2$	0.44001	6h	$C_6P_3^-$	C_s	$^1A'$	3.05396
3f	$C_3P_3^-$	C_s	$^3A''$	1.47106	6i	$C_6P_3^-$	C_s	$^1A'$	3.24934
3g	$C_3P_3^-$	C_s	$^3A''$	1.54698	6j	$C_6P_3^-$	C_s	$^1A'$	4.39168
3h	$C_3P_3^-$	C_{2v}	$^3B_1$	1.68657	7a	$C_7P_3^-$	C_{2v}	$^3B_1$	0
3i	$C_3P_3^-$	C_s	$^3A''$	2.36550	7a	$C_7P_3^-$	C_{2v}	$^1A_1$	0.59069
3j	$C_3P_3^-$	C_s	$^1A'$	2.54782	7b	$C_7P_3^-$	C_s	$^3A''$	0.19565
3k	$C_3P_3^-$	C_s	$^1A'$	3.46268	7c	$C_7P_3^-$	C_{2v}	$^1A_1$	0.73145
3l	$C_3P_3^-$	C_s	$^1A'$	3.91928	7d	$C_7P_3^-$	C_{2v}	$^1A_1$	0.81118
3m	$C_3P_3^-$	C_s	$^3A''$	4.53372	7e	$C_7P_3^-$	C_{2v}	$^1A_1$	1.06397
4a	$C_4P_3^-$	C_{2v}	$^3B_2$	0	7f	$C_7P_3^-$	C_s	$^3A''$	1.88359
4a	$C_4P_3^-$	C_{2v}	$^1A_1$	0.85214	7g	$C_7P_3^-$	C_s	$^3A''$	2.11080
4b	$C_4P_3^-$	C_s	$^3A''$	0.72274	7h	$C_7P_3^-$	C_s	$^1A'$	3.91629
4c	$C_4P_3^-$	C_{2v}	$^3B_2$	0.99486	7i	$C_7P_3^-$	C_s	$^1A'$	4.67659
4d	$C_4P_3^-$	C_s	$^3A''$	1.55106	8a	$C_8P_3^-$	C_{2v}	$^3B_2$	0
4e	$C_4P_3^-$	C_s	$^3A''$	1.64467	8a	$C_8P_3^-$	C_{2v}	$^1A_1$	1.07131
4f	$C_4P_3^-$	C_s	$^3A''$	1.76331	8b	$C_8P_3^-$	C_s	$^3A'$	0.58505
4g	$C_4P_3^-$	C_{2v}	$^1A_1$	2.00277	8c	$C_8P_3^-$	C_{2v}	$^1A_1$	1.68004
4h	$C_4P_3^-$	C_2	^1A	2.20115	8d	$C_8P_3^-$	C_s	$^3A''$	1.70263
4i	$C_4P_3^-$	C_{2v}	$^1A_1$	2.86919	8e	$C_8P_3^-$	C_s	$^3A''$	1.78943
4j	$C_4P_3^-$	C_s	$^1A'$	3.04471	8f	$C_8P_3^-$	C_{2v}	$^3A_2$	2.03434
4k	$C_4P_3^-$	C_{2v}	$^1A_1$	3.04960	8g	$C_8P_3^-$	C_{2v}	$^3B_2$	2.51707
4l	$C_4P_3^-$	C_1		3.80037	8h	$C_8P_3^-$	C_s	$^1A'$	2.80497
4m	$C_4P_3^-$	C_s	$^1A'$	4.24338	8i	$C_8P_3^-$	C_s	$^3A''$	3.83684
4n	$C_4P_3^-$	C_s	$^3A''$	4.28828	8j	$C_8P_3^-$	C_1		4.66434
					8k	$C_8P_3^-$	C_1		4.85101
					8l	$C_8P_3^-$	C_{2v}	$^3A_2$	5.20313
					8m	$C_8P_3^-$	C_s	$^1A'$	7.06604

B3LYP/6-31G* optimization. With $n > 3$, the first and the last C−C bond lengths of the C_n chain are about 1.32 Å. When n is even (i.e., in the cases of $C_4P_3^-$, $C_6P_3^-$, and $C_8P_3^-$), the straight C_n chains show an alternate long-and-short pattern in bond lengths that is similar to that of polyacetylene. When n is odd (i.e., in the cases of $C_3P_3^-$, $C_5P_3^-$, and $C_7P_3^-$), the bond

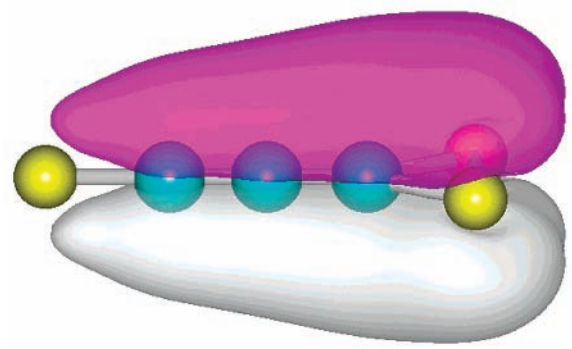

Figure 9. Schematic diagram of the $^1b_1$ molecular orbital of $C_3P_3^-$ 3D isosurface.

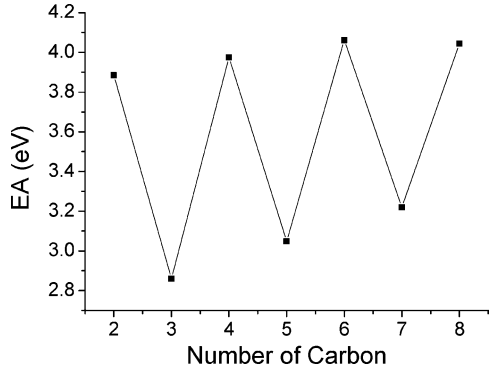

Figure 10. Curve of electron affinity (shown in Table 2) against the number of carbon atoms in $C_nP_3^-$ ($n = 2-8$).

TABLE 2: Electron Affinities (eV) with the Zero-Point Energy Correction of $C_nP_3^-$ ($n = 2-8$) that Display the Structural Style of Model 2b Based on B3LYP/6-31G* Geometries and B3LYP/6-311+G* Energies

figure	cluster	electron affinities
2b	$C_2P_3^-$	3.88487
3b	$C_3P_3^-$	2.86003
4a	$C_4P_3^-$	3.97586
5a	$C_5P_3^-$	3.04875
6a	$C_6P_3^-$	4.06166
7a	$C_7P_3^-$	3.21996
8a	$C_8P_3^-$	4.04413

lengths of the C−C bonds within the straight chain average out and are about 1.28 Å, similar to those of the cumulenic structures. As for the C−P bonds, the length is 1.60 Å when n is even, which is slightly shorter than those of $C_3P_3^-$, $C_5P_3^-$, and $C_7P_3^-$.

The incremental binding energy (ΔE^I),[9,21] which is the difference in the atomization energies (ΔE_a) of adjacent clusters, can also reflect the relative stability of the anionic clusters (Table 3). We have

$$\Delta E^I = \Delta E_a(C_nP_3^-) - \Delta E_a(C_{n-1}P_3^-)$$

where ΔE_a can be defined as the energy difference between a molecule and its component atoms:

$$\Delta E_a = nE(C) + 3E(P) - E(C_nP_3^-)$$

Figure 12 shows that, according to n, the values of ΔE^I vary alternately: when n is even, the ΔE_n value is larger; when n is odd, the ΔE_n value is smaller. Because a larger ΔE^I value implies a more stable $C_nP_3^-$ structure, one can deduce that a $C_nP_3^-$ cluster with even n is more stable than one with odd n.

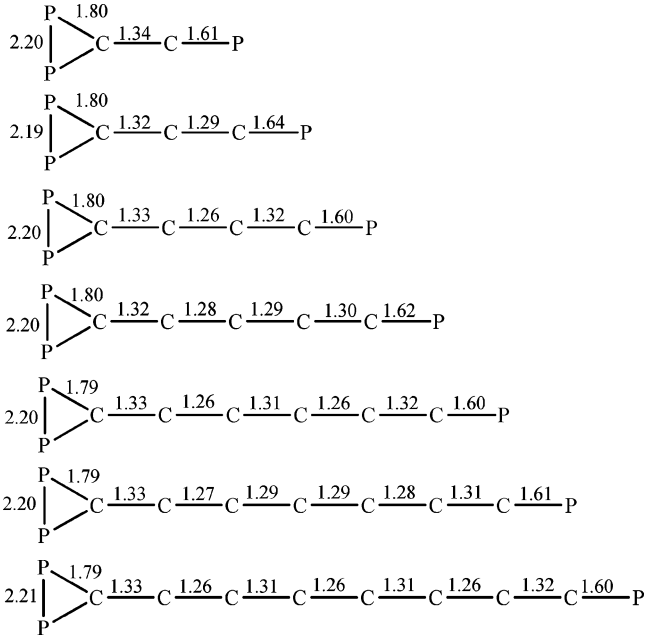

Figure 11. Bond lengths (in Å) of $C_nP_3^-$ ($n = 2-8$), which displays the structural style of model 2b after B3LYP/6-31G* optimization.

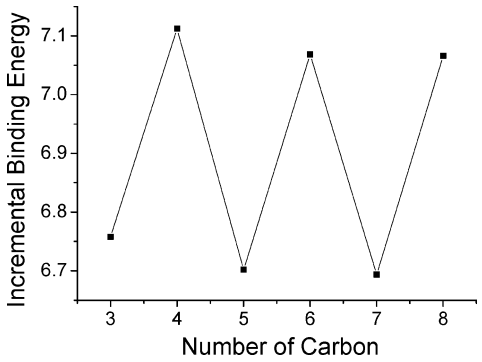

Figure 12. Curve of the incremental binding energy (ΔE^I) of $C_nP_3^-$ ($n = 3-8$) shown in Table 3.

TABLE 3: Atomization Energy (ΔE_a) and Incremental Binding Energy (ΔE^I) with the Zero-Point Energy Correction of $C_nP_3^-$ ($n = 2-8$) That Display the Structural Style of Model 2b Based on B3LYP/6-31G* Geometries and B3LYP/6-311+G* Energies

cluster	$C_2P_3^-$	$C_3P_3^-$	$C_4P_3^-$	$C_5P_3^-$	$C_6P_3^-$	$C_7P_3^-$	$C_8P_3^-$
ΔE_a	23.96778	30.72542	37.83770	44.53951	51.60754	58.30118	65.36718
ΔE^I		6.75764	7.11229	6.70160	7.06823	6.69364	7.06600

Of the 11 isomers of $C_2P_3^-$ shown in Figure 2, with a, j, and k being the exceptions, the C_2 entity can be considered to be a submolecular unit whereas the phosphorus atoms appear in P, P_2, and P_3 submolecular units. The total energy of model 2a is the lowest, and it is a chain structure with carbon and phosphorus connecting to each other alternately. Of the 13 $C_3P_3^-$ isomers shown in Figure 3, only models k, l, and m contain interconnecting carbon and phosphorus atoms, but the total energies of these isomers are high. After many calculations on $C_2P_3^-$ and $C_3P_3^-$, we found that except for several structures the isomers with interconnecting carbon and phosphorus are either unstable (with high total energy) or imaginary in frequency with no local minima. The C_nP^-, $C_nP_2^-$, $C_nP_4^-$, and $C_nP_5^-$ ($n = 3-9$) structures with carbon and phosphorus interconnecting to each other reported by Fisher et al. are also unstable.[4]

Displayed in Figure 13 are seven categories of planar structures of $C_nP_3^-$. Model 13a is the ground-state structure.

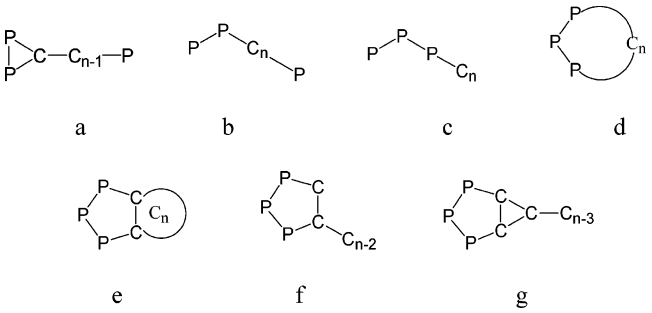

Figure 13. Seven stable models of $C_nP_3^-$ ($n = 2-8$).

Model 13b is a P_2C_nP chain structure whereas 13c is a P_3C_n chain structure. The 13d structure is a P_3C_n ring whereas 13e is composed of a P_3C_2 ring and a C_n ring sharing the same C−C edge. In the 13f structure, a P_3C_2 ring is connected to a C_{n-2} straight chain. In model 13g, a P_3C_2 ring and a C_3 ring share the same C−C edge, and the third C atom of the C_3 ring connects to a C_{n-3} straight chain. It has been pointed out before that the stable structures of small C_n clusters are either linear or cyclic[20] and that the phosphorus atoms of stable C_nP^- and $C_nP_2^-$ structures are located at the ends of the carbon chains.[7−9,12,13] Similarly, in the stable structures of $C_nP_3^-$, the phosphorus atoms are connected to stable C_n units as illustrated in Figure 13.

Acknowledgment. This work was supported by the Hong Kong Baptist University (grant FGR/01-02/I-32), the National Science Foundation of China (grant 2957117), and the Fujian Science and Technology Project of China (grant 2002F010).

Note Added after ASAP Posting. This article was released ASAP on October 24, 2003. The title of the paper has been revised. The correct version was posted on October 30, 2003.

References and Notes

(1) Bell, M. B.; Feldman, P. A.; Kwok, S.; Matthews, H. E. *Nature* **1982**, *295*, 389.
(2) Matthews, H. E.; Irvine, W. M.; Friberg, P.; Brown, R. D.; Godfrey, P. D. *Nature* **1984**, *310*, 125.
(3) Millar, T. J. *Astron. Astrophys.* **1991**, *242*, 241.
(4) Fisher, K.; Dance, I.; Willett, G. *Eur. Mass Spectrom.* **1997**, *3*, 331.
(5) Liu, Z. Y.; Huang, R. B.; Zheng, L. S. *Z. Phys. D* **1996**, *38*, 171.
(6) Liu, Z. Y.; Huang, R. B.; Huang, F.; Wang, C. R.; Zheng, L. S. *Chin. J. Chem. Phys.* **1995**, *11*, 710.
(7) Zeng, R.; Liu, J. B.; Hang, C. Y.; Gao, Z. *Chem. J. Chin. Univ.* **2000**, *21*, 581.
(8) Zhan, C. C.; Iwata, S. *J. Chem. Phys.* **1997**, *107*, 7323.
(9) Pascoli, G.; Lavendy, H. *J. Phys. Chem. A* **1999**, *103*, 3518.
(10) Pascoli, G.; Lavendy, H. *Int. J. Mass Spectrom.* **1999**, *189*, 125.
(11) Pascoli, G.; Lavendy, H. *Int. J. Mass Spectrom.* **2001**, *206*, 153.
(12) Liu, Z. Y.; Huang, R. B.; Tang, Z. C.; Zheng, L. S. *Chem. Phys.* **1998**, *229*, 335.
(13) Liu, Z. Y.; Huang, R. B.; Zheng, L. S. *Chem. J. Chin. Univ.* **1997**, *18*, 2019.
(14) del Río, E.; Barrientos, C.; Largo, A. *J. Phys. Chem.* **1996**, *100*, 585.
(15) Largo, A.; Barrientos, C.; Lopez, X.; Ugalde, J. M. *J. Phys. Chem.* **1994**, *98*, 3985.
(16) *Hyerchem Reference Manual*; Hypercube Inc.: Waterloo, Ontario, Canada, 1996; pp 79−290.
(17) James, M.; Crabbe, C.; Appleyard, J. R.; Lay, C. R. *Desktop Molecular Modeller*; Oxford University Press: Oxford, England, 1994; pp 57−124.
(18) Frisch, M. J.; Trucks, G. W.; Schlegel, H. B.; Scuseria, G. E.; Robb, M. A.; Cheeseman, J. R.; Zakrzewski, V. G.; Montgomery, J. A., Jr.; Stratmann, R. E.; Burant, J. C.; Dapprich, S.; Millam, J. M.; Daniels, A. D.; Kudin, K. N.; Strain, M. C.; Farkas, O.; Tomasi, J.; Barone, V.; Cossi, M.; Cammi, R.; Mennucci, B.; Pomelli, C.; Adamo, C.; Clifford, S.; Ochterski, J.; Petersson, G. A.; Ayala, P. Y.; Cui, Q.; Morokuma, K.; Malick, D. K.; Rabuck, A. D.; Raghavachari, K.; Foresman, J. B.; Cioslowski, J.; Ortiz, J. V.; Stefanov, B. B.; Liu, G.; Liashenko, A.; Piskorz, P.; Komaromi, I.; Gomperts, R.; Martin, R. L.; Fox, D. J.; Keith, T.; Al-Laham, M. A.; Peng, C. Y.; Nanayakkara, A.; Gonzalez, C.; Challacombe, M.; Gill, P. M. W.; Johnson, B. G.; Chen, W.; Wong, M. W.; Andres, J. L.; Head-Gordon, M.; Replogle, E. S.; Pople, J. A. *Gaussian 98*, revision A.7; Gaussian, Inc.: Pittsburgh, PA, 1998.
(19) Foresman, J. B.; Frisch, Æ. *Exploring Chemistry with Electronic Structure Methods*; Gaussian Inc.: Pittsburgh, PA, 1996.
(20) Orden, A. V.; Saykally, R. J. *Chem. Rev.* **1998**, *98*, 2313.
(21) Pascoli, G.; Lavendy, H. *Int. J. Mass Spectrom. Ion Processes* **1998**, *173*, 41.